Title
Performance of a Field-Scale Shallow Horizontal Thermal Energy Storage System

Authors
Başer, Tuğçe
Hanna, Candice
McCartney, John S

Publication Date
2019-03-21

DOI
10.1061/9780784482148.028

Peer reviewed

Performance of a field-scale shallow horizontal thermal energy storage system

Tuğçe Başer, Ph.D., A.M.ASCE[1], Candice Hanna, S.M.ASCE[2], and John S. McCartney, Ph.D., P.E., F.ASCE[2]

[1]Assistant Professor, University of Illinois at Urbana-Champaign, Department of Civil and Environmental Engineering, 205 N. Mathews, Urbana, IL 61801; e-mail: tbaser@illinois.edu.
[2]Undergraduate Researcher, University of California San Diego, Department of Structural Engineering. 9500 Gilman Dr., La Jolla, CA 92093-0085; e-mail: cfhanna@ucsd.edu.
[3]Associate Professor, University of California San Diego, Department of Structural Engineering. 9500 Gilman Dr., La Jolla, CA 92093-0085; e-mail: mccartney@ucsd.edu.

ABSTRACT

This study focuses on the performance of a shallow, horizontal thermal energy storage system in San Diego. Heat collected from solar thermal panels over a period of 120 days was injected into a slinky-loop heat exchanger installed at a depth of 1.2 m from the ground surface in compacted backfill soil, and the evolution in ground temperature was measured using embedded temperature sensors in the subsurface. Although the heat injection rate used in the experiment was relatively small, the field test still provides useful data for the validation of design models for horizontal heat storage systems. For an average heat injection rate of 20 W/m^2, the ground temperature increased to approximately 6 °C greater than the ambient ground temperature expected at the depth of the heat exchanger. An analytical model for horizontal heat exchangers considering surface temperature fluctuations was calibrated against the measured data and was used to evaluate the impacts of design parameters on the storage of thermal energy in the shallow subsurface.

INTRODUCTION

A challenge facing society is the storage of thermal energy collected from renewable sources (e.g., solar thermal panels, solar co-generation of heat and electricity, etc.) or biproducts of industrial operations (e.g., heat rejected by power plant operations, etc.) so that it can be used later for space heating or enhancing industrial processes. The subsurface soil or rock is an effective storage medium when combined with geothermal heat exchange system due to its low thermal conductivity. Claesson and Hellström (1981) introduced the concept of duct storage systems, which consist of closely-spaced geothermal heat exchangers in vertical boreholes within the subsurface installed for storing thermal energy. These systems have been adopted into practice in several locations and are now commonly referred to as borehole thermal energy storage (BTES) systems (Sibbitt et al. 2012; Nussbicker-Lux 2012; Bjoern 2013). BTES systems function similarly to conventional geothermal heat exchange systems, where a carrier fluid is circulated through a closed-loop pipe network, but with the boreholes spaced relatively close together (e.g., 1 to 2 m) to concentrate heat. Several demonstration-scale BTES systems have also been constructed to understand how the efficiency of these systems can be improved (Baser et al. 2016; McCartney et al. 2017), and the heat transfer processes in BTES systems have been simulated considering different heat transfer mechanisms (Welsch et al. 2015; Catolico et al. 2016; Baser et al. 2018). McCartney et al. (2013) proposed that BTES systems be installed in unsaturated soil layers due to their relatively lower thermal conductivity and the potential for enhancing heat transfer due to coupled heat transfer and water flow. The impact of coupled heat transfer and water flow on geothermal heat exchangers was confirmed by Baser et al. (2018), who found that heat transfer may be faster in unsaturated soils because of vapor diffusion and pore water phase change. Further, they observed permanent drying during heating of a geothermal heat exchanger, leading to a decrease in thermal conductivity and greater heat retention in the surrounding soil.

One disadvantage of BTES systems is the cost of installing closely-spaced vertical boreholes in the subsurface (Reed et al. 2018). An alternative approach is investigated in this study, where horizontal geothermal heat exchange systems are used as part of a shallow horizontal thermal energy storage (HTES) system. Horizontal geothermal heat exchange systems usually involve pipes placed in a serpentine or slinky-loop fashion within an excavation below the local depth of frost penetration, D_{frost}. The performance of horizontal geothermal heat exchange systems in different configurations have been evaluated using numerical simulations, primarily focusing on the impact of geometric variables (loop spacing, depth), surface temperature boundary conditions, soil thermal conductivity, and heat transfer rates (Fujii et al. 2012; Chong et al. 2013; Selemat et al. 2015, 2016; Zhang et al. 2017). Field tests have also been performed to evaluate their heat transfer performance in single and multiple rows (Fujii et al. 2012; Zhang et al. 2017). Most of these studies focused on diurnal heat exchange, rather than on monotonic heat injection and retention required for a heat storage system.

A schematic cross-section view of a HTES system is shown in Figure 1(a), highlighting the relevant geometric variables and important design variables. The HTES system is formed by making an excavation, possibly placing a hydraulic barrier, placing the horizontal geothermal heat exchangers having a thickness of d, and then placing backfill soil. Different from a conventional horizontal heat exchange system, backfill soil may be impounded atop the original ground surface to increase the depth of insulating backfill, d. The surface can be vegetated and may require a retention system depending on the value of d. The heat is stored in the subsurface below the level of the heat exchangers as well as within the insulating backfill, shown as an approximate volume $V_{storage}$. Stored heat may be recovered by circulation of room-temperature water through the system (direct extraction) or using a heat pump. Although less earthwork is required for HTES systems compared to BTES systems, they may be affected more by ambient surface temperature fluctuations. In a HTES system, the heat exchangers may be more closely spaced, so the insulating properties of the backfill soil and the depth of burial are critical variables for retaining heat and minimizing heat losses to the surface. HTES systems are more likely to be in unsaturated soils compared to BTES systems, which extend to a greater depth.

The expected performance of a HTES system is shown in Figure 1(b), in terms of the temperature at the level of the heat exchanger. As most shallow horizontal geothermal energy storage systems are installed at a depth that is still affected by the surface fluctuations, there will be natural ground temperature fluctuations at this depth. For a given heat injection rate, $\dot{Q}$ (W) or heat flux, $\dot{q}$ (W/m^2), the temperature at the level of the heat exchanger will be greater than that of the natural ground temperature at that depth. The heat stored would be equal to the average temperature difference from the natural ground temperature fluctuations multiplied by the volumetric heat capacity and the storage volume. Due to the greater losses from the HTES systems compared to BTES systems, it is likely that heat injection should continue throughout the year. The HTES system will store heat for a shorter period than a BTES system, but this time duration may be sufficient so that thermal energy can be used at other times from when it is generated.

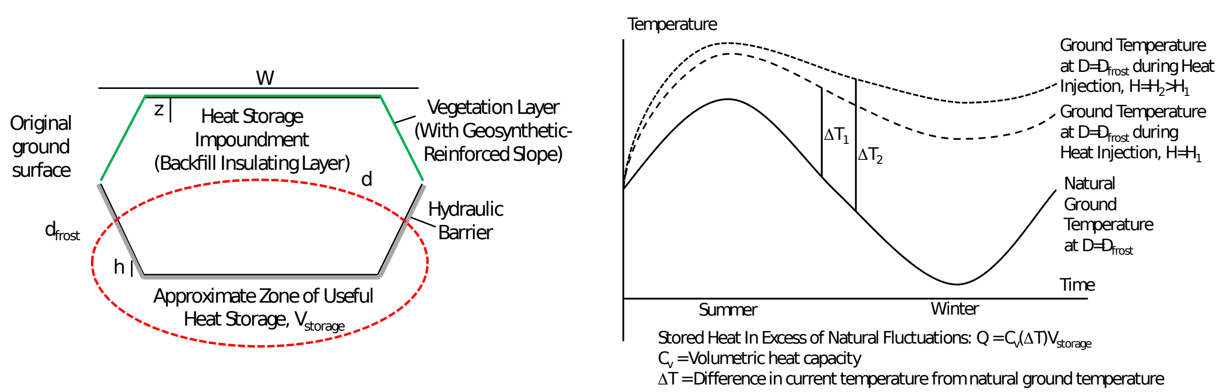

(a) (b)

Figure 1. (a) Schematic diagram of a HTES system; (b) Expected performance of a HTES system with reference to natural ground temperature fluctuations.

SHALLOW HORIZONTAL THERMAL ENERGY STORAGE SYSTEM AT UCSD

A full-scale BTES system and two HTES systems were installed at the Englekirk Structural Engineering Center (ESEC) on the UCSD campus in 2015. The performance of the BTES system was described by McCartney et al. (2017). The subsurface at the site consists of 1 m of silty sand underlain by conglomerate bedrock, with a groundwater table more than 30 m deep. The thermal conductivity of the unsaturated silty sand near the ground surface measured using the TRIM method (Lu and Dong 2015) and was found to be 1.2 W/m°C for the initial average degree of saturation of 0.6 within the top 1 m from the ground surface. The conglomerate has a relatively high hydraulic conductivity of 10^{-5} m/s, indicating that infiltration, evaporation, and coupled heat transfer and water flow will affect the HTES system performance.

The BTES systems includes a network of 25 mm-diameter high density polyethylene (HDPE) tubing installed within 15 boreholes in a hexagonal array with a spacing of 1.5 m as shown in Figures 2(a) and 2(b). Two HTES systems were installed at the site, referred to as systems H-1 and H-2 with similar configuration. The HTES were installed in excavations having dimensions of 3m × 5 m and depths of 1.2m. Both HTES systems incorporated slinky-loop heat exchangers having a length of 165 m, placed in a tighter configuration than in conventional horizontal geothermal heat exchange systems so that the thickness of the heat exchanger was approximately h = 0.1 m. HTES system H-1 included a 75 mm-thick expanded polystyrene insulation layer at a depth of 1m from the surface, while HTES system H-2 only included backfill soil. The excavations for both systems were backfilled up to the original ground surface, and a surface mound was not installed as shown in Figure 1(a). Dielectric sensors that can measure changes in both volumetric water content and temperature were installed at different depths in the HTES systems as shown in Figure 2(c). A reference borehole 9 m away from the thermal energy storage systems was used to monitor natural ground temperature fluctuations. Because the temperature response of both HTES systems H-1 and H-2 were found to be similar, indicating that the expanded polystyrene insulation layer did not have a major effect, this paper is focused on the performance of HTES system H-2. A picture of the three systems is shown in Figure 3.

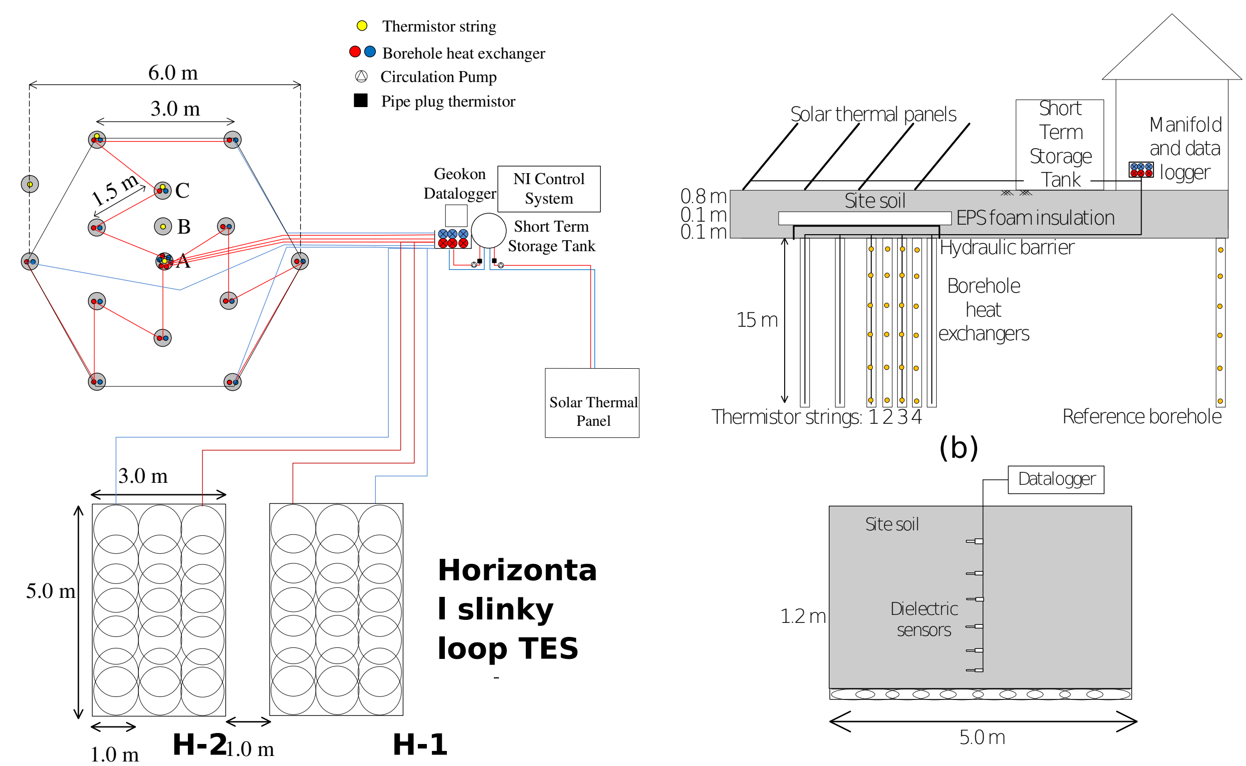

(a) (c)

Figure 2. UCSD thermal energy storage (TES) systems: (a) Plan view, (b) Elevation view of BTES system; (c) Plan view of the HTES system.

Figure 3. Picture of the UCSD thermal energy storage (TES) systems before backfilling

The air temperature at the site over an approximately two-year period is shown in Figure 4(a), while the natural ground temperature fluctuations at different depths monitored in the reference borehole over the same time period are shown in Figure 4(b). The reference borehole extends to a much greater depth than the HTES system but it still useful to understand the ambient ground temperature fluctuations. Although the sensor at a depth of 1.82 m is slightly below the depth of the excavations for the HTES system (1.2 m), it shows that temperature fluctuations of ±5 °C with an average temperature of 22 °C may occur at this depth. Below a depth of 3 m at the site the ground temperature does not fluctuate significantly. Comparison of the temperatures in Figures 4(a) and 4(b) shows that the ground temperature fluctuations are much smaller than the air temperature fluctuations due to the insulating properties of the soil.

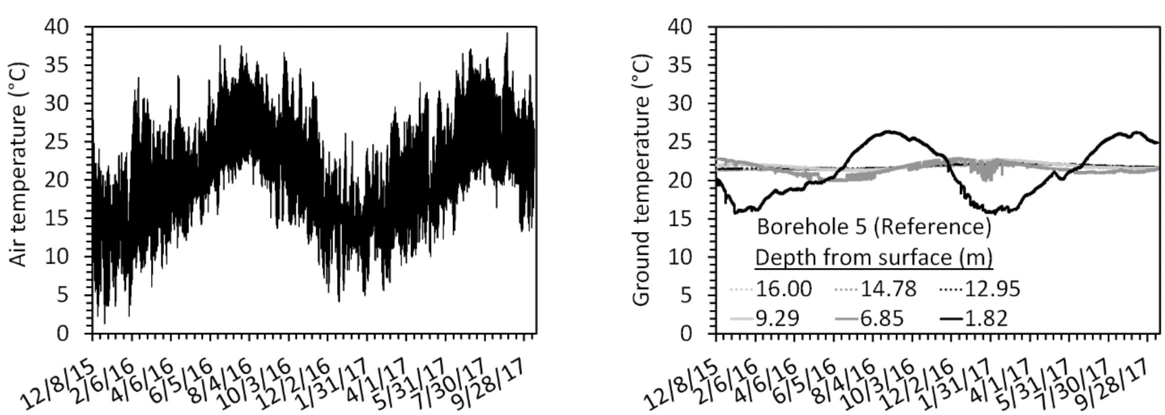

(a) (b)

Figure 4. (a) Air temperature fluctuations; (b) Natural ground temperature fluctuations.

The testing program involved a 4-month period where heat collected from solar thermal panels was injected into the BTES and HTES systems, followed by a 5-month ambient cooling period. Because the primary focus of this project was on the performance of the BTES system, the circulating fluid flow rates into HTES systems were restricted so that the majority of the thermal energy collected from the solar thermal panels was injected into the subsurface. The heat transfer rate was calculated from the following equation:

$$\dot{Q} = \dot{V}_{fluid} \rho_{fluid} c_{p,fluid} (T_{¿} - T_{out}) \qquad (1)$$

where $\dot{V}_{\text{fluid}}$ is the volumetric flow rate of the fluid circulating through the horizontal heat exchangers, ρ_{fluid} is the density of the circulating fluid (water), $c_{\text{p,fluid}}$ is the specific heat capacity of water, and T_{in} and T_{out} are in temperatures of the fluid entering and exiting the slinky-coil geothermal heat exchangers, respectively. The heat flux calculated by dividing the heat transfer rate from Eq. (1) by the gross horizontal heat exchanger area is shown in Figure 5. After an initial adjustment period where the heat flux was an average of 50 W/m^2, the volumetric flow rate was decreased to impose an average heat flux of 20 W/m^2. These correspond to heat transfer rates of 750 and 300 W, respectively. For comparison, the heat transfer rates into the BTES system during the same period were approximately 1500 W.

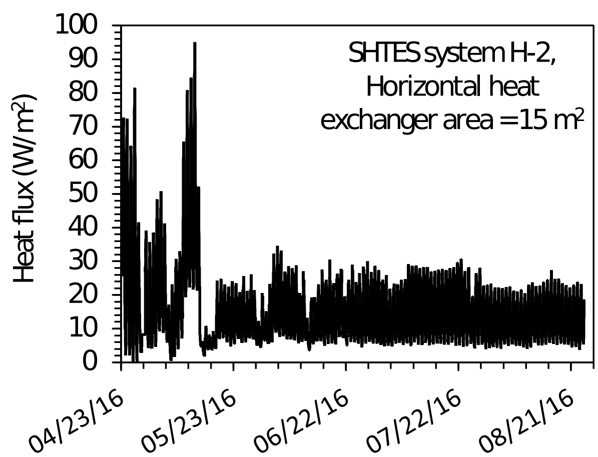

Figure 5. Heat transfer rates into HTES system H-2.

ANALYTICAL MODEL FOR HORIZONTAL HEAT EXCHANGERS

One of the goals of this study is to use the ground temperatures from the field installation to calibrate an analytical model for heat transfer into a shallow horizontal heat exchanger. Specifically, this study applies the model for 2-dimensional shallow geothermal heat exchangers (GHEs) developed by Ciriello et al. (2015). This model considers the impacts of the natural ground temperature fluctuations on the temperature in the soil around a heat exchanger for a given heat flux applied to the area of the heat exchanger. The natural ground temperature is represented using the following equation:

$$T_{nat}(z,t) = T_m - A e^{-az} \cos(\omega t - az) \qquad (2)$$

where T_m is the mean ground temperature that is constant below a certain depth, A is the yearly amplitude of thermal oscillations, z is the depth from the ground surface, t is the time in Julian days, $\omega = 2\pi/365$ is the fluctuation frequency, $a = (\omega/2\alpha)^{1/2}$, $\alpha = \lambda_{soil}\rho_{soil}/c_{p,soil}$ is the thermal diffusivity, λ_{soil} is the soil thermal conductivity, ρ_{soil} is the soil total density, and $c_{p,soil}$ is the soil specific heat capacity. The temperature at any time t, horizontal location x, and depth z can be calculated as follows:

$$T(x,z,t) = T_{nat}(z,t) + \frac{1}{4\lambda_{soil}}\sqrt{\frac{\kappa}{\pi}}\sum_{i=1}^{N} T_i(x,z,t) \tag{3}$$

where N is the number of horizontal heat exchangers, and $T_i(x,z,t)$ is defined as follows:

$$T_i = \int_{t_0}^{t} \frac{q_0(\tau)}{\sqrt{t-\tau}} \exp\left[\frac{-(x-\xi_i)^2}{4\kappa(t-\tau)}\right] \sum_{j=1}^{4} v_j \, erf\left(\frac{\psi_j}{2\sqrt{\kappa(t-\tau)}}\right) d\tau \tag{4}$$

where τ is a dummy variable for temperature, ξ_i are specific horizontal locations of the heat exchangers, $v_1 = v_4 = 1$, $v_2 = v_3 = -1$, $\psi_1 = d + z$, $\psi_2 = d - z$, $\psi_3 = d + z + h$, $\psi_4 = d - z + h$, d is the depth of burial of the heat exchanger from the surface and h is the heat exchanger thickness.

COMPARISON OF EXPERIMENTAL DATA AND ANALYTICAL MODEL RESULTS

The analytical model was first calibrated to match the soil and geometrical properties of HTES system H-2 that has a value d of 1.1 m and a value of h of 0.1 m. The locations of the two horizontal heat exchangers are shown in Figure 2(a). Subsurface temperatures recorded before heat injection were used to calibrate the model for natural ground temperature fluctuations given in Eq. (2). Example comparisons between the measured ground temperatures and the calibrated T_{nat} values at two depths are shown in Figures 6(a) and 6(b) for the model inputs in Table 1. Although the model cannot capture high frequency changes in temperature near the ground surface, the temperatures from analytical model agree well with the measured natural ground temperature fluctuations.

Table 1. Calibrated model inputs

Total density of soil, ρ_{soil}	1600	kg/m^3
Specific heat capacity of soil, $c_{p,soil}$	1300	J/kg°C
Thermal conductivity of soil, λ_{soil}	1.20	W/m°C
Mean ground temperature, T_m	21.5	°C
Annual amplitude of temperature fluctuations, A	8.0	°C

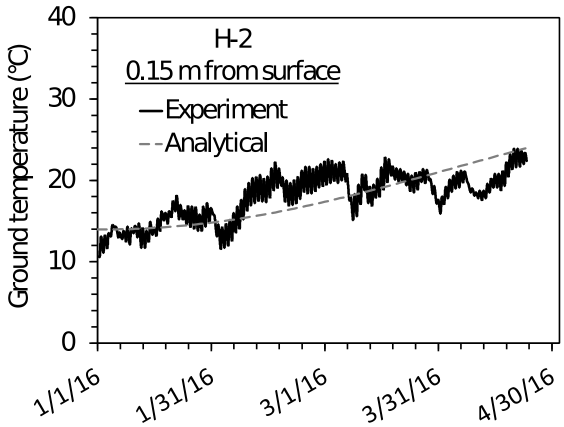

(a)

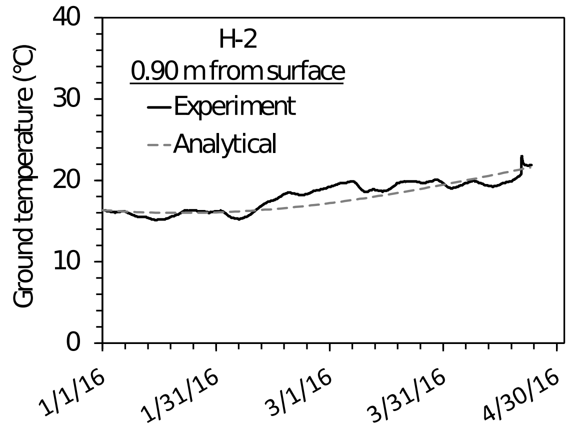

(b)

Figure 6. Natural ground temperature fluctuation calibration: (a) z=0.15 m; (b) z=0.90 m.

The temperature responses at different depths in the HTES during heat injection are shown in Figure 7. The values predicted from Eq. (3) are also shown in this figure for a heat flux of 20 W/m^2 for the full heat injection period, which only permits a qualitative comparison due to the change in heat flux at the beginning of the experiment. The maximum temperature difference between the measured ground temperature closest to the heat exchanger (depth of 0.9 m) and that estimated from the natural ground temperature fluctuation is 6 °C. Despite the use of a constant heat flux, the analytical model shows a reasonable match to the experimental data. The greater temperatures near the end of the heat injection period are not well-captured possibly due to the influence of the value of T_{nat} on the model predictions and the possibility of thermally-induced drying on the heat retention in the surface soil layer. The ground temperature increased to approximately 31 °C at the end of the heat injection period, with relatively uniform increases in temperature with depth. The natural ground temperature expected at the end of the injection period is approximately 25 °C from Eq. (2), so this indicates that the heat injection led to an increase in ground temperature of approximately 6 °C. Assuming that the volume of heat storage is 36 m^3, equal to the area of the heat exchangers (15 m^2) multiplied by a depth of 2.4 m (i.e., 1.2 m above and below the heat exchanger), 450 MJ was stored in the HTES system at the end of heat injection.

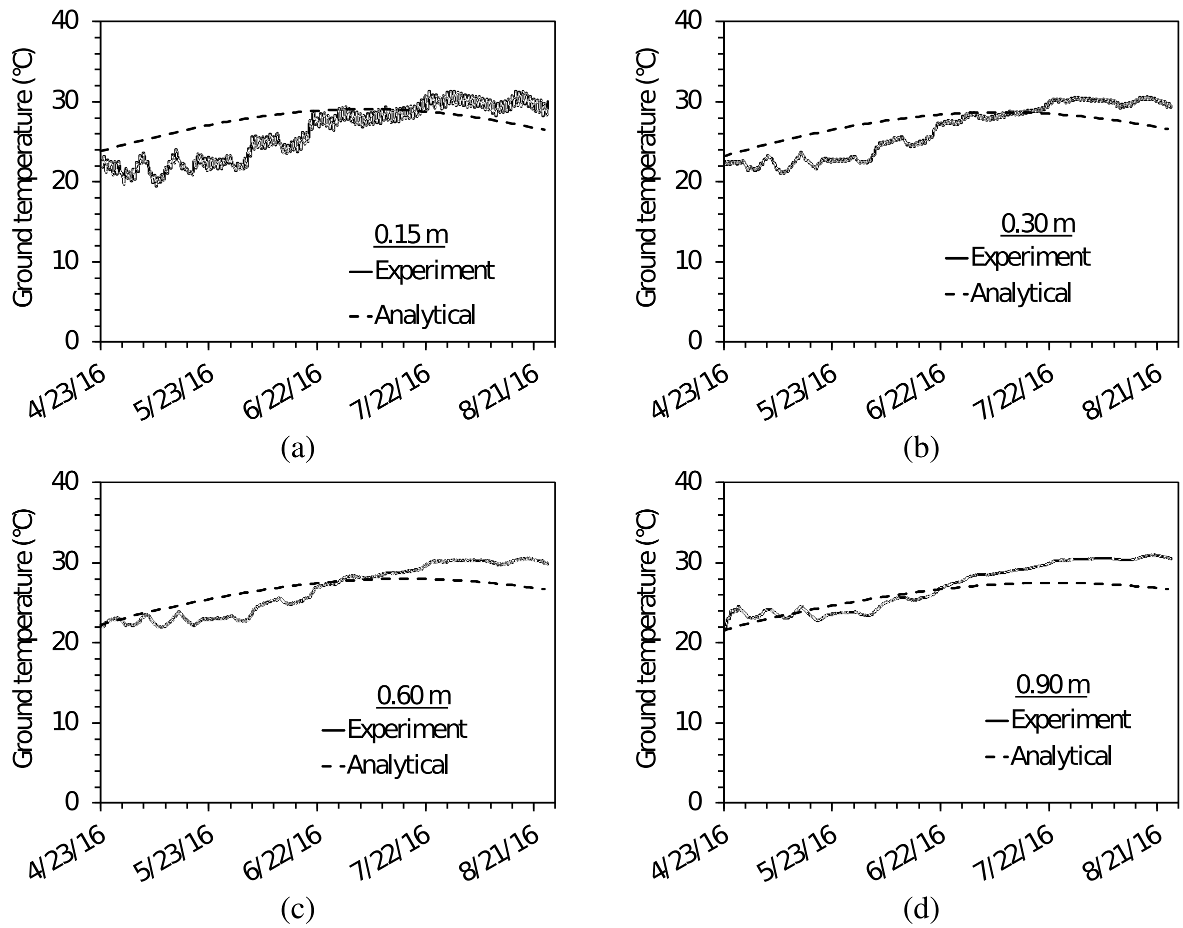

Figure 7. Examples of model calibration for the natural ground temperature fluctuations: (a) Depth of 0.15 m; (b) Depth of 0.30 m; (c) Depth of 0.60 m; (d) Depth of 0.90 m.

PARAMETRIC EVALUATION

The calibrated model can be used to evaluate the impact of different variables on the performance of HTES systems at the temperatures atop the heat exchanger (z = 1.1 m), using the same geometry and $T_{nat}(z,t)$ as the field test. Increasing the heat flux q leads to a linear increase in ground temperature within the HTES system as shown in Figure 8(a). The thermal conductivity of the backfill has a small effect on the ground temperature shown in Figure 8(b). This is possibly because the natural ground temperature fluctuations are also affected by the thermal conductivity in the model. As the analytical model cannot consider transient changes in thermal conductivity associated with thermally-induced drying, prediction of temperature response should be bounded using thermal conductivity values for saturated and dry soil. Future studies will evaluate the combined effects of the thermal conductivity and the depth of burial of the heat exchanger.

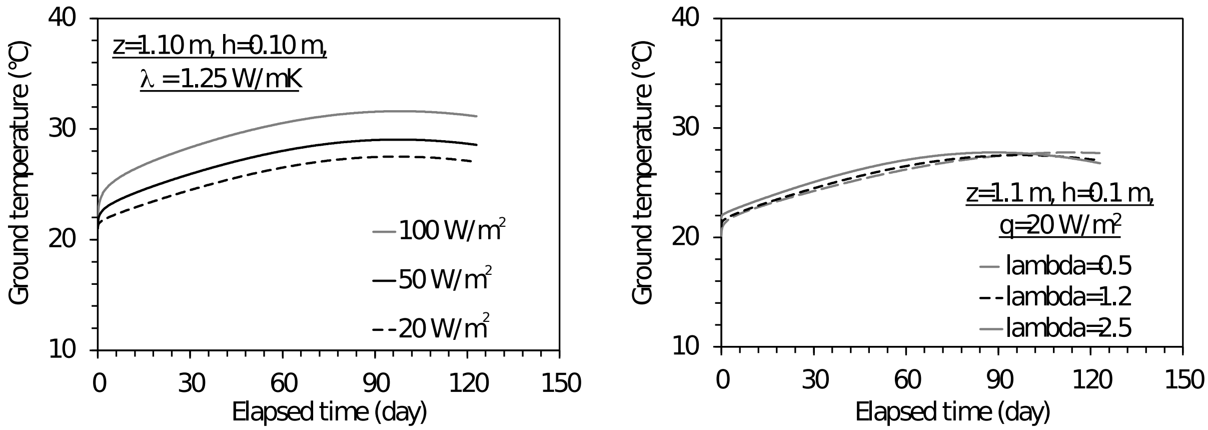

(a) (b)

Figure 8. Effect of different parameters on the temperature within a HTES system having similar characteristics/location to the site: (a) Heat flux; (b) Backfill thermal conductivity.

CONCLUSION

This study presents a comparison between the measured soil temperatures in a shallow horizontal thermal energy storage (HTES) system and those predicted from an analytical model. Reasonable agreement is observed between the predicted and measured values, indicating that the analytical model can be used for preliminary design of HTES systems. Due to the heat losses to the ground surface, it is recommended that these systems be used for short-term heat storage rather than long-term heat storage like in borehole thermal energy storage systems. It is recommended to continuously inject heat into these systems so that it may be used a short time after injection.

REFERENCES

Başer, T., Dong, Y., Moradi, A.M., Lu, N., Smits, K., Ge, S., Tartakovsky, D., and McCartney, J.S. (2018). "Role of water vapor diffusion and nonequilibrium phase change in geothermal energy storage systems in the vadose zone." *J. Geotech. Geoenviron. Eng*. 144(7), 04018038.

Başer, T., Lu, N. and McCartney, J.S. (2016). "Operational response of a soil-borehole thermal energy storage system." *J. Geotech. Geoenviron. Eng*. 142(4), 04015097.

Bjoern, H. (2013). "Borehole thermal energy storage in combination with district heating. *Proc. Euro. Geothermal Cong. 2013*. Pisa. June 3-7. 1-13.

Nussbicker-Lux, J. 2012. The BTES project in Crailsheim (Germany) – Monitoring results." Proc. of 12th Int. Conference on Energy Storage - Innostock, 16-18 May, Lleida, Spain.

Catolico, N., Ge, S., and McCartney, J.S. (2016). "Numerical modeling of a soil-borehole thermal energy storage system." *Vadose Zone Journal*. 15(1), 1-17.

Chong, C.S.A., Gan, G., Verhoef, A., Gonzalez Garcia, R., Vidale, P.L. (2013). "Simulation of thermal performance of horizontal slinky-loop heat exchangers for ground source heat pumps." *Applied Energy*. 104, 603-610.

Ciriello, V., Bottarelli M., Di Federico, V., and Tartakovsky, D.M. (2015). "Temperature fields induced by geothermal devices." *Energy*. 93, 1896-1903.

Fujii, H., Nishi, K., Komaniwa, Y., and Chou, N. (2012). "Numerical modeling of slinky-coil horizontal ground heat exchangers." *Geothermics*. 41, 55-62.

Lu, N. and Dong, Y. (2015). "A closed form equation for thermal conductivity of unsaturated soils at room temperature." *J. Geotech. Geoenviron. Eng*. 141 (6): 04015016.

McCartney, J.S., Ge, S., Reed, A., Lu, N., and Smits, K. (2013). "Soil-borehole thermal energy storage systems for district heating." *Proc. Euro. Geothermal Cong. 2013*. Pisa. pp. 1-10.

McCartney, J.S., Başer, T., Zhan, N., Lu, N., Ge, S., and Smits, K. (2017). "Storage of solar thermal energy in borehole thermal energy storage systems." *IGSHPA Technical Conference and Expo*. Denver, CO. IGSHPA. Mar. 14-17. 1-8.

Reed, A.L., Novelli, A.P., Doran, K.L. Ge, S., Lu, N., and McCartney, J.S. (2018). "Solar district heating with underground thermal energy storage: Pathways to commercial feasibility in North America." *Renewable Energy*. 126, 1-13.

Selamat, S., Miyara, A., Kariya, K. (2015). "Analysis of short time period of operation of horizontal ground heat exchangers." *Resources*. 4, 507-523.

Selamat, S., Miyara, A., Kariya, K. (2016). "Numerical study of horizontal ground heat exchangers for design optimization." *Renewable Energy*. 954, 561-573.

Sibbitt, B., McClenahan, D., Djebbar, R., Thornton, J., Wong, B., Carriere, J. and Kokko, J. (2012). "The performance of a high solar fraction seasonal storage district heating system - Five years of operation." *Energy Procedia*. 30, 856–865.

Welsch, B., Rühaak, W., Schulte, D.O., Bär, K., Homuth, S. and Sass, I. (2015). "Comparative study of medium deep borehole thermal energy storage systems using numerical modelling." In *Proc., World Geothermal Congress 2015*. Bochum, Germany: IGA. 1–6.

Zhang, C., Yang, W., Yang, J., Wu, S., and Chen, Y. (2017). "Experimental investigations and numerical simulation of thermal performance of a horizontal slinky-coil ground heat exchanger." *Sustainability*. 9(1362), 1-22.